



# Surface Energy and Lewis Acid-base Characteristics of Lignocellulosic Fibers upon Modification by Chemical Vapor Deposition of Trichloromethylsilane: An Inverse Gas Chromatography Study

J. A. F. Gamelas, M. Azpeitia, P. J. Ferreira & A. Tejado

To cite this article: J. A. F. Gamelas, M. Azpeitia, P. J. Ferreira & A. Tejado (2018) Surface Energy and Lewis Acid-base Characteristics of Lignocellulosic Fibers upon Modification by Chemical Vapor Deposition of Trichloromethylsilane: An Inverse Gas Chromatography Study, Journal of Wood Chemistry and Technology, 38:3, 264-275, DOI: [10.1080/02773813.2018.1454961](https://doi.org/10.1080/02773813.2018.1454961)

To link to this article: <https://doi.org/10.1080/02773813.2018.1454961>

 View supplementary material 

 Published online: 29 May 2018.

 Submit your article to this journal 

 View related articles 

 View Crossmark data 



## SURFACE ENERGY AND LEWIS ACID-BASE CHARACTERISTICS OF LIGNOCELLULOSIC FIBERS UPON MODIFICATION BY CHEMICAL VAPOR DEPOSITION OF TRICHLOROMETHYLSILANE: AN INVERSE GAS CHROMATOGRAPHY STUDY

J. A. F. Gamelas,<sup>1</sup> M. Azpeitia,<sup>2</sup> P. J. Ferreira,<sup>1</sup> and A. Tejado<sup>2</sup>

<sup>1</sup>Department of Chemical Engineering, CIEQPPE, University of Coimbra, Coimbra, Portugal

<sup>2</sup>Sustainable Construction Division, TECNALIA, Azpeitia, Spain

The surface of a thermomechanical pulp (TMP), containing 26 wt% of lignin, was modified by silanization with trichloromethylsilane (TCMS) via chemical vapor deposition, and thoroughly analyzed for its physicochemical properties by inverse gas chromatography (attenuated total reflection-Fourier transform infrared spectroscopy and X-ray photoelectron spectroscopy being used as complementary tools). For a 2-min TCMS-treated TMP, a decrease of the dispersive component of the surface energy from 38 to 14 mJ m<sup>-2</sup> (at 40°C), and, at the same time, an increase of the Lewis acidic and Lewis basic characters were found. The surface of this sample, modified in a high extent, was similar to that of a bleached kraft pulp (<0.1 wt% of lignin) subjected to the same silanization process, which is suggested as being due, in both cases, to the formation of a methyl-silica coating on the fiber's surface. The new silanized fibers obtained from cheap TMP can be used for the production of a new generation of biocomposites with a variety of matrices.

**KEYWORDS.** Lignocellulose, chemical vapor deposition, silanization, inverse gas chromatography, surface energy, Lewis acid-base character

### INTRODUCTION

Lignocellulosic fibers have long been used for different applications, especially as the main constituent of paper and paperboard, but also as a component in a wide variety of composite materials.<sup>[1]</sup> These fibers present different compositions and characteristics depending on the raw material and the conditions used in their production.<sup>[2,3]</sup> For instance, kraft pulping followed by bleaching renders relatively pure cellulose fibers (>85% cellulose) but at low extraction yields (ca. 50%), while thermomechanical pulping produces fibers rich in hemicelluloses (up to 20%) and lignin (ca. 25%) at a very high yield (>95%).

Lignocellulosic fibers are typically hydrophilic, including those with a high content of lignin, an aromatic polymer with a less

hydrophilic character. For example, a previous study showed a water contact angle of ca. 15° measured using the sessile drop method on a chemithermomechanical pulp (CTMP) paper with a high lignin surface content,<sup>[4]</sup> and a water contact angle of 43° was reported for a similar CTMP using the Wilhelmy plate method for single fibers.<sup>[5]</sup> Lignocellulosic fibers show thus a natural tendency to absorb water but also a very low affinity toward hydrophobic materials, that is to say, two characteristics that hamper their use in a multitude of applications. For this reason, over the last decades a lot of effort has been devoted to chemically modify the hygroscopic and polar character of cellulose fibers.<sup>[6,7]</sup>

Among the various approaches described in the literature for the hydrophobization

Address correspondence to J. A. F. Gamelas, CIEQPPE, Department of Chemical Engineering, University of Coimbra, Pólo II. R. Sílvio Lima, PT - 3030-790 Coimbra, Portugal. E-mail: [jafgas@eq.uc.pt](mailto:jafgas@eq.uc.pt)

Color versions of one or more of the figures in the article can be found online at [www.tandfonline.com/lwct](http://www.tandfonline.com/lwct).

of cellulosic materials, only a few methods lead to highly hydrophobic or even superhydrophobic surfaces, i.e., surfaces with a water contact angle above  $150^\circ$ .<sup>[3,7]</sup> Furthermore, those methods usually are either time-consuming intricate strategies or they focus almost exclusively on high-purity cellulosic fibers, in which the negative effect of the presence of the other wood components on the efficiency of these modification strategies is obviated. For instance, superhydrophobic paper was obtained by physical precipitation of carnauba wax onto the surface of cellulose fibers, upon immersion of filter paper in a chloroform solution containing the wax for 2 h and further coagulation in a water/ethanol bath for 3 h.<sup>[8]</sup> On the other hand, superhydrophobic peroxide-bleached thermomechanical pulp (TMP) paper was also obtained by combining  $O_2$  etching and plasma-enhanced chemical vapor deposition of fluorocarbon,<sup>[9]</sup> rendering chemically-bonded coatings. Likewise, an example for the superhydrophobization of lignocellulosic fibers is given by the treatment of bamboo surfaces by combining a hydrothermal process with ZnO and chemical vapor deposition (CVD) of fluoroalkyl silane at  $130^\circ\text{C}$  for 3 h.<sup>[10]</sup> Recently, softwood and hardwood surfaces were hydrophobized using a combination of  $O_2$  plasma activation and coating of pre-hydrolyzed methyltrimethoxysilane. The treatment also imparted oleophobic character to the surface of the materials.<sup>[11]</sup> Ultimately, all of these seem to be effective, yet complex multiple-step strategies.

On the other hand, as shown by the authors in previous studies<sup>[12,13]</sup> trichloromethylsilane (TCMS) is an excellent candidate for this kind of modifications. Under certain reaction conditions, homopolymerization of TCMS is conveniently favored after grafting onto the fiber's surface through the hydroxyl groups, leading to the formation of a covalently bonded nanoscale polymethylsiloxane coating.<sup>[14,15]</sup> The nonpolar character of the created layer leads to a superhydrophobic surface in a single and simple step. Different authors have reported the use of TCMS to treat cellulosic surfaces, including bleached pulp treated by immersion in TCMS solution<sup>[16]</sup> or

filter paper and cotton linters treated by means of CVD.<sup>[17,18]</sup>

In this context, the evaluation of the resultant fiber surface properties with reliable assessment tools becomes of utmost importance regarding the knowledge, understanding, and prediction of the new material's behavior.<sup>[19]</sup> With a full characterization of the surface properties, better decisions can be made regarding the fate of the materials especially in the applications where interface and adhesion issues have high relevance (e.g., composites reinforcement, specialty papers).

As detailed elsewhere,<sup>[20,21]</sup> inverse gas chromatography (IGC) represents a convenient versatile and sensitive tool to evaluate the physicochemical properties of the surface of solid materials in powder, fiber, or other forms. In brief, by using this technique, a great variety of surface parameters can be obtained for the material under analysis, including the dispersive component of the surface energy, Lewis acid-base specific components, the nanoroughness or the Flory–Huggins solubility parameters. IGC is also highly advantageous over the classical contact-angle measurements for the analysis of porous, rough, and heterogeneous surfaces, provided that the material can be packed into a column. Consequently, it has been used in the past to assess changes in the surface properties of cellulose and lignocellulosic materials occurring during functionalization reactions, e.g., esterification by acyl chlorides,<sup>[22]</sup> fatty acids<sup>[23]</sup>, or anhydrides,<sup>[24]</sup> coupling reactions with reagents containing isocyanate moieties<sup>[24,25]</sup> and chemical modifications with dichlorodiethylsilane or  $\gamma$ -aminopropyltriethoxysilane.<sup>[26–28]</sup>

In previous work, the authors successfully implemented a simple and fast CVD procedure to obtain superhydrophobic bleached kraft pulp through a 2-min exposure to TCMS vapor at ambient temperature and atmospheric pressure.<sup>[13]</sup> In addition to obtaining remarkable surface properties, as assessed by IGC analysis, the efficiency of the functionalization was found to depend on the reaction conditions, especially CVD temperature and time, parameters on which the industrial viability of this kind of processes also strongly depend.

The optimization of those parameters, together with the convenient selection of the pulp type, will ultimately shape economically and industrially viable solutions that can have a place in the market. Aligned with this statement, in the present work, TMP fibers have been subjected to CVD with TCMS and thoroughly analyzed for their physicochemical surface properties by IGC. The TMP fibers are cheaper and easier to produce than bleached kraft pulp fibers but, as mentioned above, have high lignin content which has a chemical reactivity different from cellulose. CVD conditions have been slightly varied to obtain a low and a high degree of functionalization, with the objective of exploring the efficiency of the treatment at mild conditions. The dispersive component of the surface energy at several temperatures, specific components of the free energy of adsorption of a wide range of probes, and the Lewis acid-base character of the surface have been determined, and the results critically discussed. Attenuated total reflection-Fourier transform infrared (ATR-FTIR) spectroscopy and X-ray photoelectron spectroscopy (XPS) were also used to obtain information on the chemical structure of the materials surfaces. The main purpose was thus to evaluate the extent of changes in the surface chemical properties of the TMP fibers by the CVD treatment with TCMS (in comparison to the analogous treatment of bleached kraft pulp) targeting application of the resultant materials in the composites production.

## EXPERIMENTAL

### Materials

A TMP, provided by a local paper mill was used in this study as received. The lignin content was found to be 25.8 wt% (TAPPI T222 om-02 Method) and the ash content was 1.2 wt% (TAPPI T211 om-12). Cellulose and hemicelluloses accounted for, respectively, 58.7 and 14.3 wt%, both determined using the Rowell method.<sup>[29]</sup> The carboxyl group content of the pulp was determined through conductometric titration and found to be 0.155 mmol

per g of pulp (all values expressed on a dry pulp basis).

Ethanol (absolute, 99.8% purity) and TCMS (99.0% purity) were obtained from Sigma and used without further purification. All probes for the IGC analysis were of chromatographic grade and were used as received from Sigma-Aldrich.

### TMP Silanization Via CVD

TMP silanization was carried out using a semi-continuous protocol, whose setup is schematized in Figure S1 (see supporting information section). Briefly, first, the pulp sample was solvent exchanged to ethanol five times and air-dried from this low surface tension solvent at room temperature, followed by grinding in a coffee mill for loosening of the fibers. Afterwards, the resultant fluffy pulp (in equilibrium with the moisture in the room environment) was placed in the CVD reactor while TCMS was injected into the reservoir, a sealed two-neck flask. Pre-dried and pre-heated air was used as the TCMS vapor carrier. This air goes through a silica gel column and then the inflow pipe is heated up to 50°C before the junction. At this point, three independent valves control the path that the air flow follows, either through the TCMS reservoir or directly to the reactor, enabling control over the TCMS exposure. Flow is created by a vacuum pump at the end of the line and can be regulated with a flowmeter. In this work, TCMS flow was adjusted to 1 L/min and TCMS was blown for 30 s and 2 min, in two separate experiments, in order to produce TMP pulps with a different degree of functionalization. The TCMS-air mixture is forced to pass through the reactor where the pulp samples have been placed held by a supporting basket with independent compartments which allows treating several samples at once. The reaction of TCMS with cellulose hydroxyls generates HCl gas which is continuously pumped out of the reactor and neutralized in a Dreschel bottle containing a NaOH aqueous solution. Finally, the TCMS flux is interrupted and air alone is passed through the samples until the pH of the air at the

output is neutral (ca. 20 min), which is confirmed by placing a water-damped pH paper at the exit.

The 2-min TCMS-treated TMP was characterized by its contact angle with water which was of approximately 142°.

### Spectroscopic Measurements

ATR-FTIR measurements were made in a Bruker Tensor 27 spectrometer equipped with a MKII Golden Gate ATR accessory. The spectra were recorded in the 400–4000  $\text{cm}^{-1}$  range with a resolution of 4  $\text{cm}^{-1}$  and a number of scans of 256. Background spectra were collected before every sampling.

The X-ray photoelectron spectra were recorded using a Kratos AXIS Ultra HAS equipment. High-resolution C 1s and Si 2p spectra were obtained with a step size of 0.1 eV and a dwell time of 1500 ms; O 1s spectra were obtained with a step size of 0.1 eV and a dwell time of 600 ms. Peak fitting of the high-resolution spectra was performed using Gaussian–Lorentzian peak shapes and Shirley-type background subtraction. More details can be found in Ref. 13.

### Inverse Gas Chromatography Analysis

The IGC analysis was performed using a DANI GC 1000 digital pressure control gas chromatograph equipped with a hydrogen flame ionization detector. Stainless-steel columns (0.5 m long and 0.4 cm inside diameter) were washed with acetone and dried before packing. For each analysis, 1–2 g of fibers was packed into the gas chromatograph column, before which the samples were gently milled using a coffee mill with blunt blades. The packed columns were shaped in a smooth “U” to fit the detector/injector geometry of the instrument and then conditioned overnight at 105°C, under a helium flow, before any measurements were conducted. The measurements were taken at the column temperatures of 40–55°C (with intervals of 5°C) with the injector and detector kept at 180 and 200°C, respectively. Helium was used as the carrier gas with a constant flow rate of ca. 5 mL/min. Small

quantities of vapor (<1  $\mu\text{L}$ ) of each probe taken from the vapor in equilibrium with the liquid phase (headspace) were injected into the carrier gas, allowing work to be performed under infinite dilution conditions. The probes used for the IGC data collection were *n*-pentane (C5), *n*-hexane (C6), *n*-heptane (C7), *n*-octane (C8), trichloromethane (TCM, Lewis acidic probe), dichloromethane (DCM, acidic), tetrahydrofuran (THF, basic), ethyl ether (basic), ethyl acetate (ETA, amphoteric), acetone (amphoteric), 1-pentene, 1-hexene, and 1-heptene (weak Lewis bases). Methane was used as the reference probe. The retention times were the average of three injections and were determined using the Conder and Young method.<sup>[30]</sup> The coefficient of variation in the retention time measurements was always lower than 5%.

From the probe's retention time data, the dispersive component of the surface free energy of each material ( $\gamma_s^d$ ) and the specific component of the free energy of adsorption ( $\Delta G_a^s$ ) of different Lewis acid-base probes on the surface of materials have been obtained.<sup>[20,21,31]</sup> The theoretical aspects underlying the calculation of these parameters are summarized in the supporting information section.

## RESULTS AND DISCUSSION

### Assessment of the Silanization Treatments by Spectroscopic Techniques

The silanization treatments were evaluated by ATR-FTIR and XPS measurements. The ATR-FTIR of TMP after reaction with TCMS using the 2-min protocol (experimental section) showed two well-resolved peaks at 1272  $\text{cm}^{-1}$  and 780  $\text{cm}^{-1}$ , not observed in the spectrum of the original TMP (Figure 1), attributed, respectively, to the symmetric bending vibration of methyl groups attached to silicon atoms and to the stretching vibration of Si–C bonds.<sup>[15,17]</sup> The FTIR spectrum of the sample produced using the 30-s protocol, on the other hand, was closer to that of the original TMP. For the 30-s treated sample the absorption at ca. 780  $\text{cm}^{-1}$  was barely perceptible and an absorption

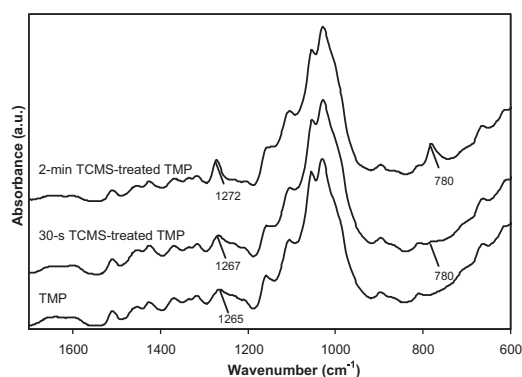


**FIGURE 1.** ATR-FTIR spectra of untreated and TCMS-treated TMP samples.

maximum in a similar frequency ( $1267\text{ cm}^{-1}$ ) of that measured in the spectrum of the initial TMP ( $1265\text{ cm}^{-1}$ ) was detected (Figure 1). These results suggest that two samples with a significantly different extent of silanization were obtained: a low degree of modification was obtained for the 30-s treated sample while for the 2-min treated sample the degree of modification was high. However, it should be noted that these assumptions refer only to the analysis of the surface of the samples up to a few micrometers depth, carried out during the ATR measurements. As for the bulk modification, the weight increase in the lignocellulosic fibers after the CVD treatment with TCMS, that can be considered an approximate quantitative measure of the degree of modification, was 0.9 wt% and 1.5 wt% for the 30-s and 2-min TCMS-treated TMP samples, respectively.

Note that for the TCMS-treated bleached kraft pulp, analyzed previously,<sup>[13]</sup> the degree of modification was 1.2 wt%.

The surface chemical composition of the TCMS-treated fibers (in comparison to the original fibers) was determined by X-ray photoelectron spectroscopy. This technique, similar to IGC, is a surface specific technique, which analyzes the surface up to a few nanometers depth. The XPS results are presented in Table 1. C and O were found as major elements and also Si was found on the surface of the treated fibers. After silanization, the atomic percentage of carbon decreased, this decrease being more pronounced for the 2-min TCMS-treated TMP. The silicon content at the surface was also higher for the material subjected to a longer treatment with TCMS. Accordingly, the Si/C atomic ratio was of 0.08 and 0.48 for the 30-s and 2-min treated TMP, respectively. These results confirm the low degree of modification (silanization) pointed out above by FTIR spectroscopy for the 30-s treated material. On the other hand, the O/C atomic ratio also increased from 0.5 in the raw material up to 1.0 in the 2-min TCMS-treated material. Chlorine, as contaminant, was only detected unambiguously for the 30-s treated TMP (ca. 0.3%, Table 1). The peak fitting of the high-resolution C 1s spectra of the different materials (Figure 2 and Table 1) revealed a large increase in the C1 component (aliphatic carbon), accompanied by the concomitant decrease in the C2 component (carbon in C–O bonds) with the

**TABLE 1.** XPS atomic percentages, atomic ratios, and results of the peak fitting of C 1s signal for TMP and TCMS-treated TMP (results of a bleached cellulosic kraft pulp, before and after silanization, are also shown for comparison).

Material	Elements (%)			Atomic ratios		C 1s components (%) <sup>a</sup>			
	C	O	Si	O/C	Si/C	C1	C2	C3	C4
TMP	67.2	32.8	—	0.49	—	35.8	52.0	10.4	1.8
30-s TCMS-treated TMP <sup>b</sup>	60.6	34.4	4.7	0.57	0.08	41.6	43.5	11.0	3.9
2-min TCMS-treated TMP	40.4	40.0	19.5	0.99	0.48	71.5	22.9	4.9	0.7
bSKP <sup>c</sup>	62.9	37.1	—	0.59	—	22.4	60.6	14.9	2.1
Sil bSKP <sup>c</sup>	39.5	41.5	19.0	1.05	0.48	65.8	27.0	6.5	0.7

<sup>a</sup>C 1s components are normalized to 100%. C1 corresponds to carbon that is linked only to hydrogen or to carbon (–C–H; –C–C, C=C), C2 corresponds to carbon that is additionally linked to a single oxygen (–C–O), C3 is due to O–C–O or –C=O bonds, and C4 is due to O–C=O bonds.<sup>[32]</sup>

<sup>b</sup>Some amount of chlorine (around 0.3%) was also detected for this sample.

<sup>c</sup>Data taken from Ref.<sup>[13]</sup>

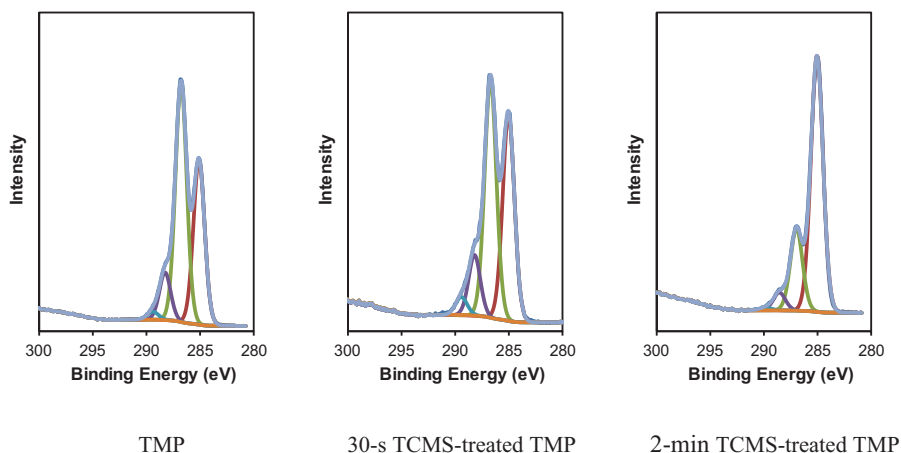


**FIGURE 2.** High-resolution XPS spectra with peak fitting in the region of carbon binding energies for TMP and TCMS-treated TMP samples.

modification process. These changes, which were more significant for the 2-min treated TMP, are an indication of the introduction of methyl groups in the cellulose chain. Following silanization, one signal was detected in the high-resolution Si 2p spectra (Figure S2, see supporting information section). The present XPS results are not substantially different from those reported previously for silanized bleached kraft pulp (bSKP, Table 1). The O/C atomic ratio was lower for the reference TMP than for the reference bSKP, as a consequence of the high content of lignin in the former.<sup>[32,33]</sup> Notwithstanding, after silanization, the surface chemical composition of both (2-min treated) TMP and bSKP was similar. Overall, it can be concluded, based on the results of FTIR and XPS that a thorough modification of the lignocellulosic pulp surface occurred in the case of the 2-min treatment with TCMS. In the case of the 30-s treatment with TCMS, the silanization was in a lesser extent. The silanization process can thus convert the surface of a lignocellulosic pulp (containing about 26% of lignin) to a methyl-silica surface, similarly to what was reported before for bleached cellulose.

#### Dispersive Component of the Surface Free Energy

The dispersive component of the surface energy of the TMP before and after its treatment with trichloromethylsilane was

determined following the Schultz and Lavielle approach.<sup>[34]</sup> The results are plotted in Figure 3. For the original TMP, the  $\gamma_s^d$  value was found to be of  $37.7 \text{ mJ m}^{-2}$  at  $40^\circ\text{C}$  with a decrease to  $33.0 \text{ mJ m}^{-2}$  at  $55^\circ\text{C}$ . After silanization, changes were noted, whose extent depended on the treated sample. For the 30-s TCMS-treated sample, the  $\gamma_s^d$  was found to decrease slightly, relatively to the original TMP: from  $37.7 \text{ mJ m}^{-2}$  to  $28.5 \text{ mJ m}^{-2}$  at  $40^\circ\text{C}$  and from  $33.0$  to  $27.6 \text{ mJ m}^{-2}$  at  $55^\circ\text{C}$ . However, for the 2-min TCMS-treated sample, the changes in the dispersive component of the surface energy in comparison to TMP were remarkably high: the  $\gamma_s^d$  value decreased to  $13.9 \text{ mJ m}^{-2}$  at  $40^\circ\text{C}$  (with  $\gamma_s^d$  values of  $13.9$

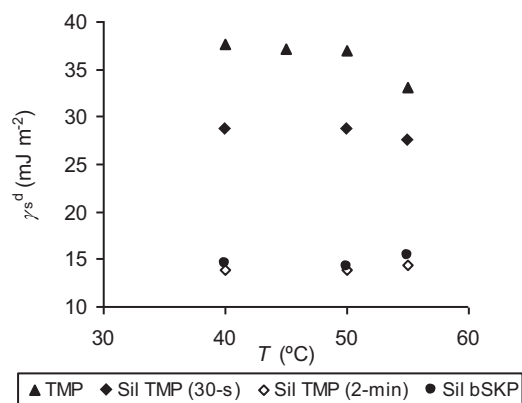


**FIGURE 3.**  $\gamma_s^d$  values at several temperatures for TMP and silanized TMP samples (results of silanized bleached kraft pulp are also shown for comparison<sup>[13]</sup>).

and  $14.5 \text{ mJ m}^{-2}$  being measured at 50 and  $55^\circ\text{C}$ , respectively). These results, in line to those reported previously for the silanization of bleached cellulosic kraft pulp (Figure 3) indicate a full functionalization of the lignocellulosic fibers surface for the 2-min TCMS-treated sample. For the 30-s treated sample the surface modification was not as significant, the results being closer to those of the original unmodified material. The introduction of methyl groups, which possess poor ability to establish London interactions, into the cellulose chains, and a lower abundance or inaccessibility of the cellulose hydroxyl groups on the surface of the functionalized lignocellulosic material, may have contributed to the overall effect of a low dispersive component of the surface energy.

There were no significant differences between the 2-min TCMS-treated thermo-mechanical pulp and the silanized bleached kraft pulp, with all values of  $\gamma_s^d$  (at the several studied temperatures) falling within the  $14\text{--}15 \text{ mJ m}^{-2}$  interval (Figure 3). This result clearly indicates that the presence of lignin in TMP had no distinct influence on the surface energy properties of the final material when a certain degree of modification was achieved. This is of particular high relevance regarding the application of these materials in the production of biocomposites: the silanization of the less costly TMP and further use of the resultant material as filler can be presented as a valid solution.

Other modifications were reported to reduce significantly (although not so remarkably) the dispersive component of the surface energy of pure cellulose, e.g., esterification or etherification reactions with incorporation of alkyl or fluorine-alkyl chains in the cellulose backbone.<sup>[22,35,36]</sup> It was also reported that the surface modification of quartz silica particles with methyltrimethoxysilane in water (with the formation of a siloxane coating) produced, as well, an impressive reduction of  $\gamma_s^d$  from the original  $255$  to  $36 \text{ mJ m}^{-2}$  for a full surface coverage by the silane.<sup>[37]</sup> Notwithstanding, the possibility of achieving such behavior by the functionalization of a lignocellulosic material, as assessed by IGC, is presented here for the first time and should be highlighted.

### Lewis Acid-Base Character

The Lewis acid-base properties of the materials were evaluated by the injection of a wide range of Lewis acidic, basic, and amphoteric probes into the IGC column. The main results for the corresponding specific interaction parameters, obtained using the Schultz and Lavielle (Figure 4) and the Dorris and Gray (Figure 5) approaches, expressed in terms of  $\Delta G_a^s$  of each probe, are summarized in Table 2.

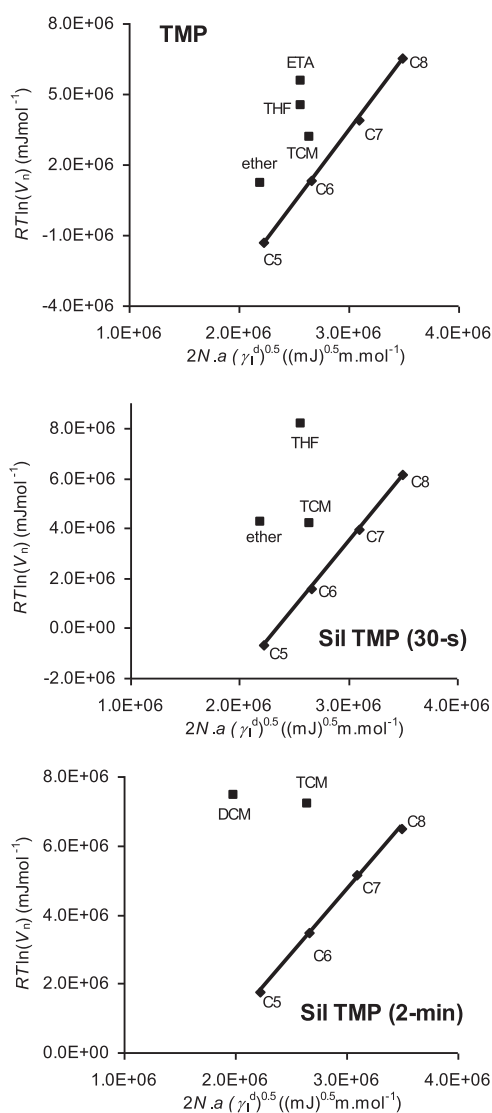
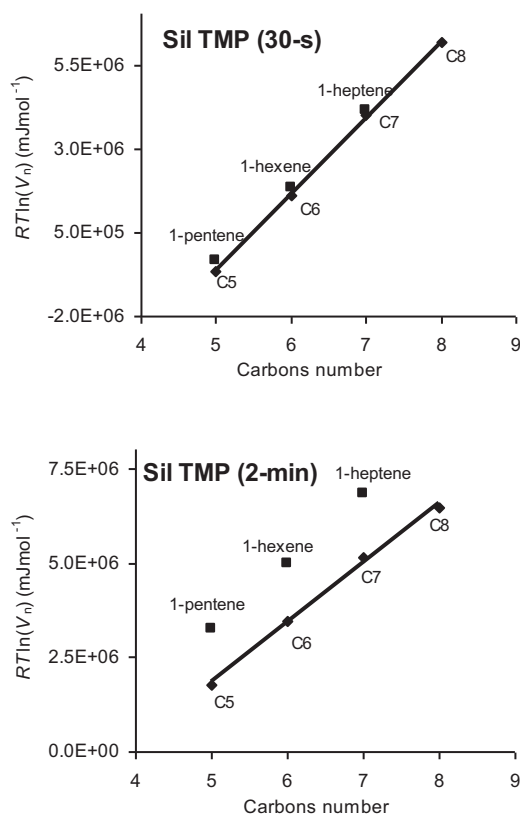


FIGURE 4. Plots of  $RT \ln(V_n)$  vs.  $2N \cdot a(\gamma_1^d)^{0.5}$  for the adsorption of *n*-alkanes and Lewis acid-base probes on TMP and silanized TMP samples (measurements at  $40^\circ\text{C}$ ).



**FIGURE 5.** Plots of  $RT\ln(V_n)$  vs. number of carbon atoms for the adsorption of *n*-alkanes and 1-alkenes on silanized TMP samples (measurements at 40°C).

The initial TMP had a dominant amphoteric character, with a slight prevalence of the Lewis acidity over the Lewis basicity, as measured by the  $\Delta G_a^s$  (THF)/ $\Delta G_a^s$  (TCM) or  $\Delta G_a^s$  (ether)/ $\Delta G_a^s$  (TCM) ratios (2.0 and 1.4, respectively, at 40°C). The specific interaction with some Lewis acid-base probes could not be measured since these provided very broad and ill-defined chromatograms (e.g., dichloromethane (DCM) and acetone). The qualitative result with acetone confirms the amphoteric character of the surface of TMP, this probe being retained irreversibly on the surface (i.e., with a too high specific interaction not possible to be measured by IGC). As for DCM, it should be noted that this probe has a molecular surface area significantly lower than the other Lewis acid-base probes used in this study.<sup>[20]</sup> Therefore, its smaller size and less steric constraints contributed to its irre-

versible retention in the stationary phase (and thus, similarly to acetone, it was not possible to measure the corresponding specific interaction by IGC). When the results of TMP are compared to those of bleached cellulosic kraft pulp, it is evident the lower Lewis acidity of TMP, as revealed by lower specific interactions with basic probes (THF, ether) and slightly higher affinity with TCM, resulting therefore in lower Lewis acidity-to-basicity ratios ( $\Delta G_a^s$  (THF)/ $\Delta G_a^s$  (TCM) ratios of 2.0 and 3.4 for TMP and bleached cellulose, respectively, at 40°C). These differences are certainly due to the fact that, besides cellulose, the TMP also contains a significant amount of lignin (26%), as a consequence of its production process. The latter confers to the surface a more bipolar character.<sup>[33]</sup>

After silanization, the Lewis acid-base characteristics of the surface of TMP changed, in an extent which was dependent on the degree of modification. Two distinct cases are present. For the 30-s TCMS-treated TMP, with a low degree of modification, a significant increase (to near the double) of the specific interactions with basic probes (THF and ether) was found, and the specific interaction with TCM also increased. Consistent results were obtained at 2 different temperatures (40 and 55°C). For the 2-min treated TMP the changes of the surface chemistry were more dramatic. The interaction with the acidic probe (TCM) increased even more and was about two times that of the original TMP (Table 2); additionally, all the typical basic and amphoteric probes (THF, ether, ETA, acetone) were retained too strongly (not eluted) on the surface of the 2-min treated TMP. These results are, thus, a clear indication that both the Lewis acidity and the Lewis basicity of the lignocellulosic material surface were increased by the silanization, the effects being more pronounced for the TMP having a higher extent of modification.

The retention times with 1-pentene, 1-hexene, and 1-heptene were also measured in order to assess any specific interaction of these weak Lewis bases with the materials surface. In contrast to the initial TMP, where the retention time (and retention volume) of a

**TABLE 2.** Specific component of the free energy of adsorption ( $-\Delta G_a^s$ , kJ mol<sup>-1</sup>) of Lewis acid-base probes on the surface of TMP and silanized TMP samples (results of a bleached cellulosic kraft pulp, before and after silanization, are also shown).

Samples	Probes								
	Acidic <sup>a</sup>		Basic <sup>a</sup>		Amphoteric <sup>a</sup> ETA	Weak basic <sup>d</sup>			$\Delta G_a^s(\text{THF})/$ $\Delta G_a^s(\text{TCM})$
	TCM	DCM	THF	Ether		1-pentene	1-hexene	1-heptene	
Untreated									
TMP (40°C)	1.90	npd <sup>c</sup>	3.78	2.71	4.81	0	0	0	2.0
TMP (55°C)	2.08	npd <sup>c</sup>	4.12	2.76	4.95	0	0	0	2.0
bSKP (40°C) <sup>b</sup>	1.56	4.37	5.33	4.70	6.12	0	0	0	3.4
TCMS-treated	Acidic <sup>a</sup>		Basic <sup>a</sup>		Amphoteric <sup>a</sup> ETA	Weak basic <sup>d</sup>			$\Delta G_a^s(\text{THF})/$ $\Delta G_a^s(\text{TCM})$
	TCM	DCM	THF	Ether		1-pentene	1-hexene	1-heptene	
Sil TMP, 30-s (40°C)	2.61	npd <sup>c</sup>	7.02	5.09	npd <sup>c</sup>	0.32	0.22	0.17	2.7
Sil TMP, 30-s (55°C)	2.90	npd <sup>c</sup>	7.16	5.15	npd <sup>c</sup>	0.41	0.31	0.10	2.5
Sil TMP, 2-min (40°C)	3.79	6.50	npd <sup>c</sup>	npd <sup>c</sup>	npd <sup>c</sup>	1.51	1.51	1.67	—
Sil TMP, 2-min (55°C)	4.11	7.04	npd <sup>c</sup>	npd <sup>c</sup>	npd <sup>c</sup>	1.17	1.27	1.21	—
Sil bSKP (40°C) <sup>b</sup>	3.37	5.02	npd <sup>c</sup>	npd <sup>c</sup>	npd <sup>c</sup>	1.01	0.98	1.01	—

<sup>a</sup>Determined using the Schultz and Lavielle approach.<sup>[34]</sup><sup>b</sup>Data taken from Ref.<sup>[13]</sup><sup>c</sup>npd = not possible to determine due to too strong retention.<sup>d</sup>Determined using the Dorris and Gray approach.<sup>[38]</sup>

specific 1-alkene was equal to that of the corresponding *n*-alkane, the retention times of the alkenes for the functionalized materials were always higher than those of the corresponding alkanes (Figure S3, see supporting information section). In fact, even for the 30-s TCMS-treated TMP sample, small but significant differences between the  $RT/\ln(V_n)$  values of 1-alkenes and of the corresponding *n*-alkanes were also measured: retention times of 1-alkenes were systematically higher under the same conditions of temperature and flow rate (Figure 5). These results revealed a specific interaction of the surface of the silanized materials with the  $\pi$  electrons of 1-alkenes. The magnitude of this specific interaction, as determined by the Dorris and Gray method, differed between the two samples of silanized TMP (Table 2). For the 30-s TCMS-treated TMP it was  $0.1\text{--}0.4 \times 10^6$  kJ mol<sup>-1</sup>, whereas for the 2-min treated TMP it was  $1.2\text{--}1.7 \times 10^6$  kJ mol<sup>-1</sup>. Furthermore, for the 30-s treated TMP, the  $-\Delta G_a^s$  (1-alkenes) decreased with the increasing chain length, i.e., 1-pentene > 1-hexene > 1-heptene. This has been already reported for other materials,<sup>[39]</sup> and suggests that, for a larger chain, there

may be a more accentuated difficulty in the orientation of the  $\pi$  electrons in the terminal of the aliphatic chain toward the acidic groups of the surface of the material, which provides the specific interaction. Overall, the results obtained by the injection of the 1-alkenes confirmed those obtained by the injection of the stronger Lewis bases: the Lewis acidity of the TMP surface was enhanced with silanization and was even more pronounced for the TMP with a higher degree of modification.

The 2-min TCMS-treated TMP showed a Lewis acid-base character similar to that of silanized bleached kraft pulp, although some slight differences could be noted. In particular, it was found that the values of the  $\pi$  interaction of 1-alkenes were ca. 1.5 times higher for silanized TMP than for silanized bleached cellulose (Table 2, 40°C).

Finally, and according to a previous determination of a nanomorphology index by IGC,<sup>[13]</sup> the variations in the Lewis acid-base character during the silanization of the lignocellulosic fibers should be mainly attributed to changes in the fiber's surface chemical structure rather than to changes in the fiber's

nanoroughness. The introduction of both basic siloxane (Si—O—Si) and acidic silanol (Si—OH) groups on the surface of the TMP may be responsible for the increase in its Lewis acid-base properties, by enhancing the formation of Lewis acid-base adducts with Lewis acidic and Lewis basic probes. Comparable results were found by IGC for the modification of quartz silica particles surface with methyltrimethoxysilane in water to produce a siloxane coating,<sup>[37]</sup> as thoroughly detailed in previous report.<sup>[13]</sup> It was proposed that the (neutral) methyl groups inserted in the siloxane chain, as they are relatively small, do not hinder (by steric hindrance) the access of the Lewis acid-base probes to the acidic and basic sites in the neighborhood of the silicon atoms to which they are attached<sup>[13,37]</sup> and thus, the acid-base properties of cellulosic pulp can even be enhanced by the coating with methyl-silica.

## CONCLUSIONS

Lignocellulosic fibers (thermomechanical pulp, TMP) reacted with trichloromethylsilane (TCMS) via chemical vapor deposition and materials with distinct surface chemical properties, as demonstrated by IGC, were obtained. Two separate treatments, differing in the contact time between the TMP and the TCMS, yielded samples with a different extent of modification. The dispersive component of the surface energy of the TMP decreased from 38 to 14 mJ m<sup>-2</sup> for the 2-min treated TMP and both the Lewis acidity and the Lewis basicity of the fibers were enhanced. These results, presented here for TMP, for the first time, are in line with those obtained for the silanization of bleached cellulosic kraft pulp by the same method and can be related, in both cases, to the formation of a methyl-silica coating on the surface of the fibers, regardless of the presence of lignin. Therefore, in spite of the different chemistry, lignin seems not to have much influence on the surface chemical properties of the final material, at least if appropriate modification conditions are chosen. In this context, it should be noted that, besides cellulose, lignin may also react with TCMS, because it also contains

hydroxyl groups (although in a lesser proportion than cellulose), through which the grafting may occur. The simultaneous very low surface energy (dispersive component) and high Lewis acid-base character of the silanized lignocellulosic fibers may be of high relevance considering their potential application in the production of new biocomposites. Additionally, the use of a thermomechanical pulp is preferable over the use of a bleached kraft pulp for the silanization modification and further application in composites, since it is cheaper and easier to obtain.

## CONFLICT OF INTEREST

The authors declare that they have no conflict of interest.

## SUPPLEMENTARY MATERIAL

Supplemental data for this article can be accessed on the publisher's website at <http://dx.doi.org/10.1080/02773813.2018.1454961>

## REFERENCES

- [1] Kalia, S.; Dufresne, A.; Cherian, B. M.; Kaith, B. S.; Avérous, L.; Njuguna, J.; Nassiopoulos, E. Cellulose-Based Bio- and Nanocomposites: A Review. *Int. J. Polym. Sci.* **2011**, *2011*, 1–35, article ID 837875. DOI: [10.1155/2011/837875](https://doi.org/10.1155/2011/837875).
- [2] Sain, M.; Li, H. Enhancement of Strength Properties of Mechanical Pulps. *J. Wood Chem. Technol.* **2002**, *2*, 187–197. DOI: [10.1081/WCT-120016257](https://doi.org/10.1081/WCT-120016257).
- [3] Dufresne, A.; Belgacem, M. N. Cellulose-Reinforced Composites: From Micro- to Nanoscale. *Polímeros* **2013**, *23*, 277–286.
- [4] Navarro, F.; Dávalos, F.; Denes, F.; Cruz, L. E.; Young, R.A.; Ramos, J. Highly Hydrophobic Sisal Chemithermomechanical Pulp (CTMP) Paper by Fluorotrimethylsilane Plasma Treatment. *Cellulose* **2003**, *10*, 411–424. DOI: [10.1023/A:1027381810022](https://doi.org/10.1023/A:1027381810022).
- [5] Gellerstedt, F.; Gatenholm, P. Surface Properties of Lignocellulosic Fibers Bearing Carboxylic Groups. *Cellulose* **1999**, *6*, 103–121. DOI: [10.1023/A:1009239225050](https://doi.org/10.1023/A:1009239225050).

- [6] Belgacem, M. N.; Gandini, A. Surface Modification of Cellulose Fibers. In *Monomers, Polymers and Composites from Renewable Resources*; Belgacem, M. N., Gandini, A., Eds.; Elsevier Science, Oxford, UK, Chapter 18, **2008**; pp 385–400.
- [7] Gandini, A.; Belgacem, M. N. The Surface and In-Depth Modification of Cellulose Fibers. *Adv. Polym. Sci.* **2016**, *271*, 169–206.
- [8] Li, P.; Li, H.; Yang, J.; Meng, Y. Facile Fabrication of Superhydrophobic Paper with Excellent Water Repellency and Moisture Resistance by Phase Separation. *Bioresources* **2016**, *11*, 6552–6565. DOI: [10.15376/biores.11.3.6552-6565](https://doi.org/10.15376/biores.11.3.6552-6565).
- [9] Mirvakili, M. N.; Hatzikiriakos, S. G.; Englezos, P. Superhydrophobic Lignocellulosic Wood Fiber/Mineral Networks. *ACS Appl. Mater. Interfaces* **2013**, *5*, 9057–9066. DOI: [10.1021/am402286x](https://doi.org/10.1021/am402286x).
- [10] Li, J.; Sun, Q.; Yao, Q.; Wang, J.; Han, S.; Jin, C. Fabrication of Robust Superhydrophobic Bamboo Based on ZnO Nanosheet Networks with Improved Water-, UV-, and Fire-Resistant Properties. *J. Nanomaterials* **2015**, *2015*, 1–9. article ID 431426.
- [11] Tang, Z.; Xie, L.; Hess, D. W.; Breedveld, V. Fabrication of Amphiphobic Softwood and Hardwood by Treatment With Non-fluorinated Chemicals. *Wood Sci. Technol.* **2017**, *51*, 97–113. DOI: [10.1007/s00226-016-0854-9](https://doi.org/10.1007/s00226-016-0854-9).
- [12] Tejado, A.; Alam, M. N.; Chen, W. C.; van de Ven, T. G. M. Superhydrophobic Foam-Like Cellulose Made of Hydrophobized Cellulose Fibres. *Cellulose* **2014**, *21*, 1735–1743.
- [13] Gamelas, J. A. F.; Salvador, A.; Hidalgo, J.; Ferreira, P. J.; Tejado, A. Unique Combination of Surface Energy and Lewis Acid-base Characteristics of Superhydrophobic Cellulose Fibres. *Langmuir* **2017**, *33*, 927–935. DOI: [10.1021/acs.langmuir.6b03970](https://doi.org/10.1021/acs.langmuir.6b03970).
- [14] Artus, G. R. J.; Jung, S.; Zimmermann, J.; Gautschi, H.-P.; Marquardt, K.; Seeger, S. Silicone Nanofilaments and Their Application as Superhydrophobic Coatings. *Adv. Mater.* **2006**, *18*, 2758–2762. DOI: [10.1002/adma.200502030](https://doi.org/10.1002/adma.200502030).
- [15] Li, S.; Xie, H.; Zhang, S.; Wang, X. Facile Transformation of Hydrophilic Cellulose into Superhydrophobic Cellulose. *Chem. Commun.* **2007**, 4857–4859. DOI: [10.1039/b712056g](https://doi.org/10.1039/b712056g).
- [16] Tang, Z.; Li, H.; Hess, D. W.; Breedveld, V. Effect of Chain Length on the Wetting Properties of Alkyltrichlorosilane Coated Cellulose-Based Paper. *Cellulose* **2016**, *23*, 1401–1413. DOI: [10.1007/s10570-016-0877-2](https://doi.org/10.1007/s10570-016-0877-2).
- [17] Cunha, A. G.; Freire, C.; Silvestre, A.; Neto, C. P.; Gandini, A.; Belgacem, M. N.; Chaussy, D.; Beneventi, D. Preparation of Highly Hydrophobic and Lipophobic Cellulose Fibers by a Straightforward Gas-Solid Reaction. *J. Colloid Interface Sci.* **2010**, *344*, 588–595. DOI: [10.1016/j.jcis.2009.12.057](https://doi.org/10.1016/j.jcis.2009.12.057).
- [18] Liao, Q.; Su, X.; Zhu, W.; Hua, W.; Qian, Z.; Liu, L.; Yao, J. Flexible and Durable Cellulose Aerogels for Highly Effective Oil/Water Separation. *RSC Adv.* **2016**, *6*, 63773–63781. DOI: [10.1039/C6RA12356B](https://doi.org/10.1039/C6RA12356B).
- [19] Gardner, D. J.; Oporto, G. S.; Mills, R.; Samir, M. A. S. A. Adhesion and Surface Issues in Cellulose and Nanocellulose. *J. Adhes. Sci. Technol.* **2008**, *22*, 545–567. DOI: [10.1163/156856108X295509](https://doi.org/10.1163/156856108X295509).
- [20] Santos, J. M. R. C. A.; Guthrie, J. T. Analysis of Interactions in Multicomponent Polymeric Systems: The Key-Role of Inverse Gas Chromatography. *Mater. Sci. Eng. R.* **2005**, *50*, 79–107. DOI: [10.1016/j.mser.2005.07.003](https://doi.org/10.1016/j.mser.2005.07.003).
- [21] Gamelas, J. A. F. The Surface Properties of Cellulose and Lignocellulosic Materials Assessed by Inverse Gas Chromatography: A Review. *Cellulose* **2013**, *20*, 2675–2693. DOI: [10.1007/s10570-013-0066-5](https://doi.org/10.1007/s10570-013-0066-5).
- [22] Gauthier, H.; Coupas, A.; Ville-magne, P.; Gauthier, R. Physicochemical Modifications of Partially Esterified Cellulose Evidenced by Inverse Gas Chromatography. *J. Appl. Polym. Sci.* **1998**, *69*, 2195–2203. DOI: [10.1002/\(SICI\)1097-4628\(19980912\)69:11%3c2195::AID-APP11%3e3.0.CO;2-Z](https://doi.org/10.1002/(SICI)1097-4628(19980912)69:11%3c2195::AID-APP11%3e3.0.CO;2-Z).
- [23] Jandura, P.; Riedl, B.; Kokta, B. V. Inverse Gas Chromatography Study on Partially Esterified Paper Fiber. *J. Chromatogr. A* **2002**, *969*, 301–311. DOI: [10.1016/S0021-9673\(02\)00892-0](https://doi.org/10.1016/S0021-9673(02)00892-0).
- [24] Trejo-O'Reilly, J. A.; Cavaille, J. Y.; Belgacem, M. N.; Gandini, A. Surface

Energy and Wettability of Modified Cellulosic Fibres for Use in Composite Materials. *J. Adhesion* **1998**, *67*, 359–374. DOI: [10.1080/00218469808011117](https://doi.org/10.1080/00218469808011117).

[25] Botaro, V. R.; Gandini, A. Chemical Modification of the Surface of Cellulosic Fibres. 2. Introduction of Alkenyl Moieties via Condensation Reactions Involving Isocyanate Functions. *Cellulose* **1998**, *5*, 65–78. DOI: [10.1023/A:1009216729686](https://doi.org/10.1023/A:1009216729686).

[26] Felix, J. M.; Gatenholm, P.; Schreiber, H. P. Controlled Interactions in Cellulose-Polymer Composites. 1: Effect on Mechanical Properties. *Polym. Compos.* **1993**, *14*, 449–457. DOI: [10.1002/pc.750140602](https://doi.org/10.1002/pc.750140602).

[27] Matuana, L. M.; Woodhams, R. T.; Balatinecz, J. J.; Park, C. B. Influence of Interfacial Interactions on the Properties of PVC/Cellulosic Fiber Composites. *Polym. Compos.* **1998**, *19*, 446–455. DOI: [10.1002/pc.10119](https://doi.org/10.1002/pc.10119).

[28] Matuana, L. M.; Balatinecz, J. J.; Park, C. B.; Woodhams, R. T. Surface Characteristics of Chemically Modified Newsprint Fibers Determined by Inverse Gas Chromatography. *Wood Fiber Sci.* **1999**, *31*, 116–127.

[29] Pettersen, R. C. The Chemical Composition of Wood. In *The Chemistry of Solid Wood*; Rowell, R. M., Ed.; American Chemical Society, Washington, D.C., Chapter 2, **1984**; pp 57–126.

[30] Kamdem, D. P.; Riedl, B. Inverse Gas Chromatography of Lignocellulosic Fibers Coated With a Thermosetting Polymer: Use of Peak Maximum and Conder and Young Methods. *J. Colloid Interface Sci.* **1992**, *150*, 507–516. DOI: [10.1016/0021-9797\(92\)90219-C](https://doi.org/10.1016/0021-9797(92)90219-C).

[31] Mukhopadhyay, P.; Schreiber, H. P. Aspects of Acid–Base Interactions and Use of Inverse Gas Chromatography. *Colloids Surf.*

A. **1995**, *100*, 47–71. DOI: [10.1016/0927-7757\(95\)03137-3](https://doi.org/10.1016/0927-7757(95)03137-3).

[32] Belgacem, M. N.; Czeremuskin, G.; Sapiuha, S.; Gandini, A. Surface Characterization of Cellulose Fibres by XPS and Inverse Gas Chromatography. *Cellulose* **1995**, *2*, 145–157. DOI: [10.1007/BF00813015](https://doi.org/10.1007/BF00813015).

[33] Shen, W.; Parker, I. H. Surface Composition and Surface Energetics of Various Eucalypt Pulps. *Cellulose* **1999**, *6*, 41–55. DOI: [10.1023/A:1009268102404](https://doi.org/10.1023/A:1009268102404).

[34] Schultz, J.; Lavielle, L.; Martin, C. The Role of the Interface in Carbon Fibre-Epoxy Composites. *J. Adhesion* **1987**, *23*, 45–60. DOI: [10.1080/00218468708080469](https://doi.org/10.1080/00218468708080469).

[35] Sasa, B.; Odon, P.; Stane, S.; Julijana, K. Analysis of Surface Properties of Cellulose Ethers and Drug Release From Their Matrix Tablets. *Eur. J. Pharm. Sci.* **2006**, *27*, 375–383. DOI: [10.1016/j.ejps.2005.11.009](https://doi.org/10.1016/j.ejps.2005.11.009).

[36] Rani, P. R.; Ramanaiah, S.; Reddy, K. S. Lewis Acid-Base Properties of Cellulose Acetate Butyrate by Inverse Gas Chromatography. *Surf. Interface Anal.* **2011**, *43*, 683–688. DOI: [10.1002/sia.3514](https://doi.org/10.1002/sia.3514).

[37] Harding, P. H.; Berg, J. C. The Role of Adhesion in the Mechanical Properties of Filled Polymer Composites. *J. Adhes. Sci. Technol.* **1997**, *11*, 471–493. DOI: [10.1163/156856197X00039](https://doi.org/10.1163/156856197X00039).

[38] Dorris, G. M.; Gray, D. G. Adsorption of n-Alkanes at Zero Surface Coverage on Cellulose Paper and Wood Fibres. *J. Colloid Interface Sci.* **1980**, *77*, 353–362. DOI: [10.1016/0021-9797\(80\)90304-5](https://doi.org/10.1016/0021-9797(80)90304-5).

[39] Pedrosa, J.; Gamelas, J. A. F.; Lourenço, A. F.; Ferreira, P. J. Surface Properties of Calcium Carbonate Modified with Silica by Sol-Gel Method. *Colloids Surf. A.* **2016**, *497*, 1–7. DOI: [10.1016/j.colsurfa.2016.02.020](https://doi.org/10.1016/j.colsurfa.2016.02.020).